

A dip-and-read impedimetric electrochemical sensor for orthophosphate monitoring

Geisianny Moreira

Clemson University

Alex B. Shaw

Arizona State University

Nafisa Amin

North Carolina State University

Wei Gao

North Carolina State University

Eric McLamore

emclamo@clemson.edu

Clemson University

Research Article

Keywords: Phosphate sensor, reagent-free sensing, P sorbent, environmental monitoring, dip-and-read sensor.

Posted Date: July 31st, 2024

DOI: https://doi.org/10.21203/rs.3.rs-4691772/v1

License: © 1 This work is licensed under a Creative Commons Attribution 4.0 International License.

Read Full License

Additional Declarations: No competing interests reported.

Abstract

Phosphorus (P) is an essential element for all life forms and a finite resource. P cycle plays a vital role in regulating primary productivity, making it a limiting nutrient for agricultural production and increasing the development of fertilizers through extractive mining. However, excessive P may cause detrimental environmental effects on aquatic and agricultural ecosystems. As a result, there is a pressing need for conservation and management of P loads through analytical techniques to measure P and precisely determine P speciation. Here, we explore a new 2D sorbent structure (GO-PDDA) for sensing orthophosphate in agueous samples. The sorbent mimics a group of phosphate-binding proteins in nature and is expected to bind orthophosphate in solution. Laser-induced graphene (LIG) was coated with GO-PDDA using a drop-cast method. Electrochemical impedance spectroscopy was used as a transduction technique for electrochemical sensing of orthophosphate (HPO_4^{2-}) and selectivity assay for chloride, sulfate and nitrate in buffer at pH 8. The analytical sensitivity was estimated to be 347 ± 90.2 Ω /ppm with a limit of detection of 0.32 ± 0.04 ppm. Selectivity assays demonstrate that LIG-GO-PDDA is 95% more selective for ortho-P over sulfate and 80% more selective over chloride and nitrate. The developed sensor can be reused after surface regeneration with an acidic buffer (pH 5), with slight changes in sensor performance. Our results show that the sorbent structure is a promising candidate for developing electrochemical sensors for environmental monitoring of orthophosphate and may provide reliable data to support sustainable P management.

Introduction

Phosphorous (P) plays an important role in biological systems and is crucial for a variety of central tasks (metabolism, genetic information exchange, cell wall integrity, etc.). However, in the wrong form excessive P may cause detrimental environmental effects on aquatic ecosystems [1] and/or agricultural systems [2, 3]. In biological systems, phosphate plays a vital role in regulating primary productivity, making it a limiting nutrient for agricultural production [4]. For this reason, the widespread use of chemical fertilizers is mainstay (particularly after the Green Revolution in the 1960s), increasing the development of P-based fertilizers through extractive mining [5]. Indiscriminate use of phosphate-based fertilizers can increase P load into water bodies, leading to environmental problems such as eutrophication and expediting water deterioration [6]. While P is ubiquitous in natural systems, much of the excess P in aquatic systems is in a form that is not bioavailable to plant uptake. Abundance of P is clearly a problem, but at the same time scarcity of the finite resource phosphorous and lack of viable recovery/reuse techniques have created a paradox [7], making P management among the biggest environmental/agricultural challenges of the 21st century. Furthermore, access to P controls food security and limits geographical access since the largest reservoirs of P are found in a few countries, generating global shortages [8]. As mined P is a finite resource, the expectation is that fertilizer prices will increase over the years, and disruption of supply chains may ensue as P mines are depleted [8]. As a result, there is a pressing need for conservation and management of P, including recovery and reuse. One of the major problems from a monitoring perspective is that there are few reliable field sensors for

quantification of P in near real-time. Thus, analytical techniques to measure P are sorely needed, and precise determination of P speciation is vital and important to guarantee precision agriculture and wastewater monitoring, for example.

Analytical methods for detection and characterization of P are classified into five distinct categories: *i*) chemical techniques (e.g., ion chromatography, inductively coupled plasma mass spectrometry, colorimetry/spectrophotometry, flow injection analysis, chromatography, and gradient thin film detection), *iii*) biological techniques (e.g., enzymatic assays, protein labeling, electrophoresis), *iiii*) molecular techniques (e.g., Raman scattering, nuclear magnetic resonance), *iv*) staining techniques (e.g., fluorescence, GFP-activated cell sorting), and *v*) chemosensors/biosensors (e.g., electrochemical, optical, magnetic transduction methods) [9]. These analytical methods vary widely in terms of efficacy, accessibility, analysis cost, need for sample pre-treatment, and requirement for trained personnel. Furthermore, the ideal analytical method used may change depending on sample matrix (e.g., aqueous or soil sample), P species of interest, and required resolution (e.g., limit of detection and detection). Chemosensors and biosensors provide advantages such as portability (in-field measurement). Optical sensors have been widely explored by Dr. Wolfbeis' lab [10] for phosphate sensing, providing insightful inputs for sensing phosphates. However, there is a critical need to enhance the sensitivity, selectivity, limit of detection, and reusability, and development cost for electrochemical sensors targeting P [11].

P has a plethora of different chemical/biochemical forms (in fact, there are thousands), making guantification and characterization challenging. More than 80% of these forms are organic P, and only a small fraction of inorganic P is water-soluble. Ortho-P is the most readily bioavailable form of dissolved inorganic P and may take one of four forms depending on pH (PO_4^{3-} , HPO_4^{2-} , $H_2PO_4^{-}$, H_3PO_4) [12]. Monitoring ortho-P in environmental, agricultural, and ecological studies is of upmost importance. Most plants uptake the primary form of ortho-P (HPO₄²⁻), although the secondary form (H₂PO₄⁻) is also bioavailable to roots [13]. To prevent eutrophication, a maximum allowable contaminant level (MCL) for total phosphorous (TP) of 0.05 to 0.1 mg-TP/L in water has been set by the U.S. Environmental Protection Agency (EPA) in some states, but adoption of total phosphorus criteria in the US has been slow even when MCL is established [14]. However, monitoring TP concentrations with high spatiotemporal resolution is a challenge. The most widely used test for estimating TP is the standard EPA spectrophotometric-based (Method 365.5) [15]. This reagent-based test requires the addition of an exogenous reagent containing ammonium molybdate, antimony potassium tartrate and acid (usually ascorbic, sulfuric or hydrochloric). The reaction converts soluble reactive phosphorus (SRP) to an antimony-phosphomolybdate complex known as a Keggin ion [16]. The elegance of the test lies in the specificity toward SRP as well as the intense color change that can be easily detected. Testing procedures rooted in Keggin ion formation are among the most selective tests for P and are central to water quality laboratories. However, not all research questions are relevant to the restrictions of the testing protocol. For example, most tests based on *Keggin ion* formation require at least 10 min of reaction time and the addition of reagents and strong acids. Reagent-free chemosensors with a high specificity toward at least one form of ortho-P (ideally primary and/or secondary) would enable high

spatiotemporal mapping, enabling new research questions that are based on rapid analysis of ortho-P and other forms of labile P in natural systems. Finally, there is a need for dip-and-read systems that can target one or more forms of P in water samples.

Electrochemical phosphate detection has emerged as a viable approach for ortho-P monitoring due to its potential for portability and miniaturization, allowing in-field deployment. Several studies have been reported for ortho-P detection using different recognition schemes, transduction techniques, P species, and reporting a wide range of limit of detection and sensitivity. For example, a Zinc(II)-dipicolylamine-modified gold electrode was applied for testing phosphate anions ($H_2PO_4^-$), based on redox activity pyridine units complexed with Zinc, with a LOD of 7.5×10^{-16} M [17]. However, acidification is needed to perform measurements at pH 4, which will require the addition of reagents for environmental water analysis. In another example, molybdate(VI) anions were immobilized within a chitosan matrix deposited on a glassy carbon electrode for phosphate anions (mainly $H_2PO_4^-$, H_3PO_4 and HPO_4^{2-}), reporting a sensitivity of $4.4 \pm 0.1 \,\mu$ A/ μ M and a LOD of $0.15 \,\mu$ M [18]. The sensing principle is based on the reduction of molybdate(VI) anions, which requires the addition of reagents to acidify the sample to pH 2. As another example, a cobalt film on glass was formed via physical vapor deposited for ortho-P sensing ($H_2PO_4^-$) at pH 4 [19], which a limit of detection estimated to be $\sim 10^{-7}$ M. Among the various electrochemical techniques, the most common include cyclic voltammetry (CV), square wave voltammetry (SWV), and DC-potential amperometry (DCPA) [20].

Laser induced graphene (LIG) is one emerging platform that is gaining much interest in chemosensing and biosensing. LIG is a one-step, facile and scalable approach to fabricated 3D porous graphene electrodes by direct writing on commercial polyimide (PI) films under ambient conditions by using a CO₂ infrared laser [21]. LIG-based electrochemical sensors are simple and cost-effective, beyond the advantage of LIG being a material with high electrical conductivity [21]. LIG can be functionalized with the material of interest (recognition element), where changes in the electrochemical response of LIG occur due to the chemical interaction between the recognition element and target analyte in solution. In the last decade since the discovery of LIG, this material has been used for targeting a wide variety of sensors, for example: bacteria [22], viruses [23], sugars [20], and ions [24]. This material is simple to fabricate, and numerous portable devices have been developed using custom form factors that meet sampling needs. Recently, a nano copper-decorated LIG chemosensor for organophosphorus pesticide (glyphosate) was developed by Bahamon-Pinzon et al [25]. To date, there are no manuscripts for detection of inorganic phosphate using LIG.

In this paper, we evaluate a new chemosensor material for targeting ortho-P in water samples based on a 2D sorbent structure (graphene oxide PolyDADAMAC, a.k.a. GO-PDDA). The nanocarbon-polymer hybrid sorbent mimics a group of phosphate-binding proteins and is synthesized using grafting techniques [26]. Based on sorption studies, the material is expected to bind ortho-P across a pH range of 5 to 9 via a combination of electrostatic interactions and hydrogen bonds. The suspended GO-PDDA material has demonstrated ability to be regenerated under acidic conditions (*manuscript in progress*).

Here, we fabricate and test LIG electrodes coated with GO-PDDA sorbent. We tested numerous electrochemical techniques and found that electrochemical impedance spectroscopy (EIS) produced the most reliable results and that the LIG-GO-PDDA electrode surface may be regenerated for ortho-P sensing. We also evaluated selectivity towards other anions (chloride, nitrate, and sulfate). This work is the first analysis of GO-PDDA sorbent as a coating material for development of a reagent-free ortho-P chemosensor.

Experimental section

Materials and reagents

Kapton[™] film (electrical grade polyimide film, 0.005" thick) was obtained from McMaster-Carr (Elmhurst, IL, USA). Potassium ferrocyanide [K₄Fe(CN)₆] and potassium ferricyanide [K Fe(CN)] were obtained from Thermo Fisher Scientific (Waltham, MA, United States). Potassium chloride (KCl), phosphate standard solution (KH PO in H O 1000 mg/l PO), nitrate standard solution (NaNO in H O 1000 mg/l NO), chloride standard solution (NaCl in H O 1000 mg/l Cl), and sulfate standard solution (Na SO in H O 1000 mg/l SO) were purchased from Sigma Aldrich (St. Louis, MO, United States). Sodium chloride/sodium bicarbonate (NaCl/NaHCO₃) solution was obtained from a local store.

Fabrication of laser-induced graphene (LIG) electrode

Our proposed sensor was based on carbon electrodes. A three-electrode plug-and-play system was fabricated using the laser-induced graphene (LIG) technique, as described in the protocol [27]. LIG three-electrode system (LIG-chip) was engraved on a Kapton film substrate using a CO_2 laser (VLS2.30DT, Universal Laser Systems, Inc., Scottsdale, AZ, US) at 75% speed, 40% power, and 1000 PPI. LIG-chip includes a reference electrode, an auxiliary electrode, and a working electrode as a whole system. The working electrode is composed of a circular working area (3.0 mm) connected to a stem (14.3 x 2 mm) leading to a bonding pad area (2.9 x 2.5 mm). A reference electrode was developed by attaching a metal adhesive tape (nickel alloy). Counter electrode is a bare LIG. A metallic tape was incorporated into the bonding pad area of all three LIG electrodes. A nitrocellulose passivation layer was applied to the stem area of all electrodes. To build the sensor in a chip format, the three-electrode system was attached to a chemical-resistant PVC (11.7mm) as physical support using double-sided tape to enable its connection to a USB connector.

LIG functionalization with graphene-oxide PolyDADMAC (GO-PDDA)

The 2D sorbent structure (PDDA) grafted graphene oxide (GO) was used as a coating material in the LIG-chip working electrode for electrochemical sensing of ortho-P in a buffer. The sorbent structure (PDDA) mimics a group of phosphate-binding proteins (PBPs) in nature and is expected to bind phosphate. Graphene oxide (GO) was used as a nucleation substrate for the polymer sorbent portion. GO-PDDA was

integrated into LIG electrodes by drop-casting 10 μ l of a GO-PDDA solution (1 mg/ml in DI water). Drop-casting was repeated three times after completely drying, resulting in the LIG-GO-PDDA surface type.

To perform electrochemical characterization before (LIG-bare) and after (LIG-GO-PDDA) functionalization with GO-PDDA, cyclic voltammetry (CV) was conducted in a redox solution (100 mM KCl, 2.5 mM $K_3[Fe(CN)_6]$, and 2.5 mM $K_4[Fe(CN)_6]$) with a potential range from – 0.8 to 0.8 V at different scan rates of 10, 20, 25, 30, 50, 100, 150, 200 mV/s. Scanning electron microscopy (SEM) and energy-dispersive X-ray spectroscopy (EDS) were performed at the Clemson University Electron Microscopy Facility using a scanning electron microscope SU5000 with an accelerating voltage of 10.8 kV to study the morphology and elemental composition of LIG-bare and LIG-GO-PDDA electrodes. Zeta potential and particle size of GO-PDDA were determined in DI water (pH 7), NaCl/NaHCO $_3$ (pH 8), KCl (pH 6) and Tris (pH 7) using a Malvern Zetasizer Nano ZS instrument (Malvern Panalytical, United Kingdom) at the Biomaterials Engineering and Testing Core Facilities at Clemson University, Clemson, SC.

Electrochemical measurements

All electrochemical measurements were carried out in a benchtop MultiPalmSens4 potentiostat (PalmSens, Houten, Netherlands). All analytical experiments were performed in a sodium chloride/sodium bicarbonate (NaCl/NaHCO₃) solution, pH 8, at 22°C and 1 atm. Due to P speciation dependent on pH, our experiments were performed at pH 8, with the predominant ortho-P species being $\mathrm{HPO_4^{2^-}}$. Electrochemical impedance spectroscopy (EIS) was adopted as a transducer technique for ortho-P detection. Cyclic voltammetry (CV) was also tested as a transduction technique, and methodological details and results can be found in the supplemental material. Sensing experiments were performed in a dip-and-read format by immersing the LIG-GO-PDDA sensor in the sodium chloride/sodium bicarbonate solution, followed by the gradual injection of analyte solution to be tested for sensitivity (HPO₄²⁻, ortho-P) and selectivity (chloride - Cl⁻, nitrate - NO³⁻, and sulfate - SO₄²⁻), with electrochemical measurement after each injection. Specifically, aliquots of analyte working solution (100 ppm) were successively injected into the electrochemical cell (15 ml of sodium chloride/sodium bicarbonate solution) in order to obtain concentrations of 0, 0.01, 0.2, 0.4, 0.6, 0.8, and 1 ppm. EIS testing was conducted with a frequency range of 0.01 Hz - 10,000 Hz, AC amplitude of 0.01 V, and a DC voltage of 0.45 V. Each analyte addition generated a change in electrochemical signal, which was recorded using the MultiTrace software (PalmSens, Houten, Netherlands). To test sensor reusability, the LIG-GO-PDDA sensor used in the first ortho-P sensing for calibration curves had the surface regenerate to reuse. Briefly, after storage for two weeks, the sensor surfaces were rinsed with DI water, followed by a rinse with acidic buffer (pH 5), and then DI water. Then, a new calibration experiment was performed by using ortho-P standard solution as previously described.

Data analysis

Electroactive surface area (ESA, mm²), oxidation peak current (i, μ A) and area between curve (ABC, C) were evaluated as a response variable from CV output during the functionalization step. From EIS testing, impedance (Ω) and capacitance (μ F) were used as a response variable using a single-frequency,

radiometric, or multi-frequency analysis. The 3.3σ method was applied to obtain the limit of detection [28]. Analytical sensitivity was calculated as the slope of the calibration curve in the dynamic concentration range where the behavior is approximately linear. All the data analysis was performed using the OriginLab software.

Results and Discussion

Material characterization

LIG-bare electrodes and LIG modified with GO-PDDA were characterized in terms of morphology using scanning electron microscopy (SEM) and electrochemical properties using cyclic voltammetry. In addition, zeta potential was determined for GO-PDDA in different solutions. Overall, GO-PDDA characterization showed a zeta potential of 46.4 ± 1.4 mV in DI water (pH 7), 28.1 ± 2.6 mV in Tris (pH 7), 17.3 ± 0.8 mV in NaCl/NaHCO₃ (pH 8), and 2.5 ± 1.7 mV in KCl (pH 6). Zeta potential measurements indicate the surface charge of particles and stability in suspension [29]. GO-PDDA zeta potential in DI water was greater than ± 30 mV demonstrating the strongly cationic property of the material in DI water [29], which can improve interactions with the negative charge of orthophosphate through electrostatic interactions. Our zeta potential results confirmed the previous characterization of GO-PDDA, demonstrating the highly positive charge responsible for the ionic interaction and hydrogen bonding with orthophosphate in the solution (*manuscript in progress*).

Figure 1A shows a representative voltammogram comparing LIG-bare and LIG-GO-PDDA during the functionalization step. Integrating GO-PDDA into the LIG working electrode increases charge storage capacity (capacitance), demonstrated by an increase in the area between curve (Fig. 1B). In addition, GO-PDDA increases conductivity of LIG demonstrated by an increase in oxidation current peak (Fig. 1B) and electroactive surface area (**Fig S1**). The SEM micrograph of the LIG-bare and LIG-GO-PDDA are shown in Fig. 1C-D. According to the EDS analysis, the LIG-bare surface is composed of 100% carbon, whereas the LIG-GO-PDDA surface is composed of 81.8% carbon, 5% oxygen, 10.3% chloride, and 0.9% sodium. Chloride and sodium are components of the buffer solution used during CV testing in the functionalization step. SEM-EDS cannot detect the polymer portion of the GO-PDDA material. GO-PDDA was previously characterized by FTIR analysis (*manuscript in progress*). Despite the background noise signal, the FTIR spectrum demonstrated the organic content of GO-PDDA material, which characteristics peaks and fingerprint when compared with GO spectrum.

Orthophosphate electrochemical sensing

For the proposed phosphate sensor, electrochemical impedance spectroscopy was used to examine the LIG-GO-PDDA sensor response to the presence of ortho-P ($\mathrm{HPO_4}^{2^-}$) within the 0 to 1 ppm concentration range in a sodium chloride/sodium bicarbonate solution (pH 8). EIS tests yield data on total impedance (Z), real impedance (Z'), imaginary impedance (Z"), total capacitance (C), real capacitance (C'), and imaginary capacitance (C") at 63 cutoff frequencies within the frequency range of 0.01 to 10,000 Hz.

From EIS data output, impedance and capacitance were suitable response variables to evaluate the sensor response to increasing ortho-P concentrations (Fig. 2). Based on impedance and capacitance, ortho-P detection seems frequency dependent, showing better detection power and signal-to-noise ratio in the frequency range from 0.01 to 1 Hz, with an optimum cutoff frequency of 0.4 Hz (**Fig S2**).

For impedance, an increase in sensor response is observed (Fig. 2B). As expected, when analyzing capacitance, a decrease in signal is observed (Fig. 2D). Both impedance and capacitance showed a sensor-to-sensor variation amongst replicates, where capacitance was highly variable compared to impedance. The sensor-to-sensor variation amongst replicates can be attributed to the in-house carbon electrodes fabrication process, which can insert variability due to the porous property of the carbon material, as observed in our previous works [22–24, 30, 31]. However, it is worth mentioning that we used a quality control (QC) process to check functionality of electrodes and select triplicates for our experiments based on similarity of electrochemical characteristics [30]. The QC process developed by Qian et al. [30] reduces the batch-to-batch variability during LIG electrode fabrication. However, the sensor functionalization step by drop-casting the GO-PDDA solution may alter the electrochemical behavior of the electrodes, increasing the sensor-to-sensor variation since its distribution is not homogenous and/or controlled. Due to less variability, better detection power, and a high signal-to-noise ratio, impedance was adopted as a response variable over capacitance for most of the analysis.

The capacitive response of LIG-bare and LIG-GO-PDDA to increasing concentrations of ortho-P is shown in Fig. 3A. The capacitive response of LIG-bare was not significantly affected by the presence of ortho-P in the buffer (Fig. 3A, black curve). However, for LIG-GO-PDDA, a positive linear correlation was obtained in response to increasing concentrations of ortho-P in the buffer (Fig. 3A, red curve). These findings demonstrate that the sensor output comes from an interaction between GO-PDDA on the LIG surface and the orthophosphate present in the solution. It has been modeling that the principle of the chemical interaction between GO-PDDA and ortho-P is based on ionic interaction and hydrogen bonds. The performance parameters for the two LIG surface types (LIG-bare and LIG-GO-PDDA) are shown in the panel **3B**. The comparison between the two surface types demonstrates linearity (R² = 0.92) in the LIG-GO-PDDA surface with lower LOD and high sensitivity when compared with LIG-bare.

Figure 4 shows the calibration curve and performance metrics for LIG-GO-PDDA sensors in response to increasing concentrations of ortho-P in the buffer. Sensors were calibrated individually and showed a similar positive linearity trend for impedance response (Fig. 4A). The error bars in the calibration curve based on mean measurements (Fig. 4B) show higher variability across replicates, which may be caused by the sensor functionalization process, as mentioned before. This observation is valid for both variables, capacitance and impedance. These findings indicate that for deployment, each sensor needs to be individually calibrated, regenerate the surface and then used in a sample, reported as ion conditioning, which is a common method for ion-selective electrodes [32, 33].

Effect of different ions on LIG-GO-PDDA sensor

We challenged the developed sensor against common ions in aqueous samples to check for interferences that could mislead the ortho-P quantification in real samples. The selectivity of the LIG-GO-PDDA sensor was evaluated against chloride (Cl $^-$), sulfate (SO $_4^{2-}$), and nitrate (NO $_3^{3-}$) since those ions coexisted with phosphate in most environmental aqueous samples [34]. Figure 5 shows selectivity performance of LIG-GO-PDDA towards phosphate, chloride, nitrate, and sulfate (equimolar concentrations) using a multivariate frequency analysis based on two cutoff frequencies (0.8 Hz/1.0 Hz). The most important feature is the ability to sense ortho-P over other tetrahedral oxyanions (SO $_4^{2-}$). We adopted this approach due to the frequency-dependent nature of the sensor detection for different ions. The developed sensor showed 80% selectivity for phosphate over nitrate and chloride and over 95% selectivity over sulfate. Even though ions can interfere with the impedimetric sensor response, it didn't show linearity, demonstrating that the sensor output for ions other than ortho-P doesn't result from analyte affinity. It is worth mentioning that the selectivity performance test was performed in the absence of phosphate, with an individual calibration curve for each ion. Sensor response to phosphate may change in a complex sample with different concentrations of mentioned ions. However, our results give a general idea of what to expect when measuring orthophosphate in a complex media.

Table 1 presents the key performance indicators for LIG-GO-PDDA sensor using the optimum cutoff frequency for orthophosphate detection ($0.4\,Hz$). The limit of detection (LOD) and sensor sensitivity are $0.32\pm0.04\,ppm$ and $347\pm90.2\,\Omega/ppm$, respectively. The LOD of the sensor is slightly above the standard recommended limit established by the USEPA to control eutrophication in environmental water. The US-EPA standard limits for total phosphate vary from $0.05\,ppm$ to $0.1\,for$ total phosphates in streams that enter lakes and total phosphorus in flowing waters, respectively [35]. Nevertheless, our results prove the potential of GO-PDDA sorbent as a coating material for reagent-free orthophosphate sensing with a response time of less than 30 minutes. In addition, due to the simple design proposed here, the LIG-GO-PDDA sensor is easy to develop, facilitating its deployment for in-field monitoring. However, future research is needed to describe the sensor operation mechanism and optimize the limit of detection and selectivity performance of the sensor for in-field deployment.

Table 1
Key performance indicators using impedance as the response variable. Multivariate frequencies (0.01 to 1 Hz) were used to calculate performance metrics (n = 5).

Performance indicator	Impedance (Ω)
Sensitivity	347 ± 90.2 Ω/ppm
Corr. Coeff. (R ²)	0.95
LOD	0.32 ± 0.04 ppm
Operation range	0.1 to 1.0 ppm
Selectivity over Chloride	80% more selective ($R^2 = 0.64$)
Selectivity over Sulfate	95% more selective ($R^2 = 0.46$)
Selectivity over Nitrate	80% more selective ($R^2 = 0.45$)

Reusability of LIG-GO-PDDA sensors

One of the properties of the GO-PDDA material is its ability to be regenerated when exposed to both alkaline and acidic solutions and reused again as an ortho-P sorbent in solution (*manuscript in progress*). We evaluated this assumption on the LIG coated with GO-PDDA. LIG-GO-PDDA sensors used previously (Fig. 4) had the surface regenerated with an acidic buffer (pH 5) after being stored for two weeks from the first ortho-P testing. After surface regeneration, LIG-GO-PDDA sensors were tested for ortho-P detection in the previously described conditions.

Figure 6 describes the performance comparison of sensors before and after the surface regeneration with an acidic buffer. Figure 6A shows a representative calibration curve for ortho-P sensing before (black) and after (red) surface regenerations. An expected positive linear response is observed in both cases; however, after surface regeneration, the sensitivity slightly decreases and the limit of detection increases (Fig. 6B).

Our results demonstrate the reusability of LIG-GO-PDDA sensors for ortho-P detection in buffer conditions. Despite decreases in sensitivity, the sensor presents the potential to be reused, which can decrease the cost of ortho-P monitoring, increasing spatiotemporal or in-situ monitoring. However, future research is needed to confirm our findings and evaluate sensor performance in environmental water. Our preliminary results contribute to the field of materials research, amplifying the potential applications of sorbents for sensor development.

Comparison with other chemosensors

The novelty of the developed chemosensors is the use of an ortho-P sorbent as a coating material for inhouse LIG electrodes. The LOD of the developed chemosensor is slightly higher than other electrochemical sensors reported in the literature (Table 2). However, while we are proposing an

innovative material for ortho-P sensing, most of the sensors in the literature are using materials well characterized for their affinity towards ortho-P. For instance, molybdate is widely used for spectrophotometric detection of ortho-P using the molybdenum blue (MB) reaction [16]. Molybdate anions can be reduced in the presence of ortho-P, and this interaction can be easily detected using voltammetric techniques [18]. Another important novelty of the developed chemosensor is the use of inhouse LIG electrodes instead of commercial electrodes, which can reduce the cost of deployment in the future. Commercial electrodes, especially gold ones, are well-known for their electrochemical properties, including high conductivity and reproducibility, and have been demonstrated as a suitable platform for ortho-P detection [17]. However, the proposed chemosensor was designed to provide accessibility and affordability for stakeholders, and using in-house electrodes may compromise sensor performance features but can provide widely deployable technology for environmental monitoring of orthophosphates. Unlike other sensors in Table 2, the LIG-GO-PDDA uses electrochemical impedance spectroscopy (EIS) as a transduction technique. EIS has been shown to be a suitable technique for detecting the interactions between GO-PDDA and ortho-P, resulting from ionic interaction and hydrogen bonding with orthophosphate in the solution. Finally, while the LOD is above the standard recommended limit established by the USEPA to control eutrophication in environmental water, it is still useful as a first effort to develop a reagent-free and dip-and-read chemosensor for ortho-P monitoring. Both LOD and sensitivity can be improved in further research.

Table 2
Key performance indicators of chemosensors for the detection of orthophosphate.

Working electrode	Transduction technique	LOD (ppm)*	Selectivity**	Reference
Glassy carbon electrode coated with Molybdate(VI) anions immobilized in a chitosan matrix	Square Wave Voltammetry	0.01	Chloride and nitrate ions	[18]
Glass printed electrode coated with Cobalt	Cyclic voltammetry and amperometry	0.01	NR	[19]
Gold electrodes coated with Dipicolylamine-zinc(II) complexes	Cyclic voltammetry	0.1	Sulfate anions	[17]
lon selective electrode coated with copper phosphate membrane	Potentiometric	0.1	Carbonate, nitrate, chloride and sulfate	[33]
Laser-induced graphene electrodes coated with graphene oxide PolyDADAMAC	Electrochemical impedance spectroscopy	0.32	Chloride, sulfate and nitrate	This work.
* LOD values were transformed t	to ppm in order to facilit	ate compari	son.	

Conclusions

A dip-and-red electrochemical sensor was developed for reagent-free orthophosphate detection. The sensing platform comprises laser-induced graphene electrodes (LIG) coated with graphene oxide PolyDADAMAC sorbent material. Electrochemical impedance spectroscopy (EIS) testing in a sodium chloride/sodium bicarbonate (NaCl/NaHCO₃) solution at pH 8 was used as detection technique. The exposure of LIG-GO-PDDA sensor to orthophosphate (HPO_4^{2-}) results in an increase of total impedance. Minimum signal changes are detected for LIG without GO-PDDA (LIG-bare) in the presence of ortho-P in the buffer. This finding demonstrates that the changes in sensor output are related to chemical interactions between GO-PDDA on the LIG surface and ortho-P in solution. LIG-GO-PDDA sensor analytical sensitivity was estimated to be 347 \pm 90.2 Ω/ppm with an estimated limit of detection of 0.32 ± 0.04 ppm in an operation range of 0.1 to 1 ppm. The selectivity assays demonstrate that LIG-GO-PDDA is 95% more selective for ortho-P over sulfate and 80% more selective over chloride and nitrate. The developed sensor can be reused after surface regeneration with an acidic buffer (pH 5), with slight changes in sensor performance (analytical sensitivity and LOD). Future work is needed to improve sensor performance regarding sensitivity, selectivity, and reproducibility. While the limit of detection of the sensor is above U.S.-EPA regulations, the major advantages of the LIG-GO-PDDA sensor presented herein are relatively facile manufacturing process, versatility in deployment in both in-laboratory and infield settings by using dip-and-read format, and reagent-free sensing. The proposed sensor has an innovative concept of using a sorbent as a coating material, bridging the material research field to the sensor development. The proposed sensor may potentially be used for pollution monitoring and/or precision agriculture after its performance metrics are improved.

Declarations

Competing interests

The authors declare no competing interests.

Funding

This work was supported by the Science and Technologies for Phosphorus Sustainability (STEPS) Center, a National Science Foundation Science and Technology Center (CBET-2019435). Any opinions, findings, and conclusions or recommendations expressed in this piece are those of the author(s) and do not necessarily reflect the views of the National Science Foundation.

Author Contribution

All authors contributed to the study conception and design. Material preparation, data collection and analysis were performed by Geisianny Moreira, Nafisa Namin and Alex Shaw. The first draft of the

manuscript was written by Geisianny Moreira, and all authors reviewed and edited previous versions of the manuscript. Funding was acquired by Wei Gao and Eric McLamore. This work was performed under supervision of Wei Gao and Eric McLamore. All authors read and approved the final manuscript.

Acknowledgement

This manuscript is dedicated to Dr. Otto Wolfbeis. As a graduate student in the early 2000's working on fiber optic sensors, Dr. McLamore's first reading assignment in a class was, what is now, a classic by Dr. Wolfbeis (DOI: 10.1021/ac060490z). Not by coincidence, the next five manuscripts which directed OUR optical sensor research were all from Dr. Wolfbeis' lab. The compelling and articulate manuscripts written by Dr. Wolfbeis and team will always be an inspiration to our team, as scientists, and as explorers. His team's work on ion selectivity and fluorescent labels e.g., chameleon) continues to drive research and will likely do so for years to come. We are honored to write a manuscript in his honor and his legacy will always live on in our lab.

References

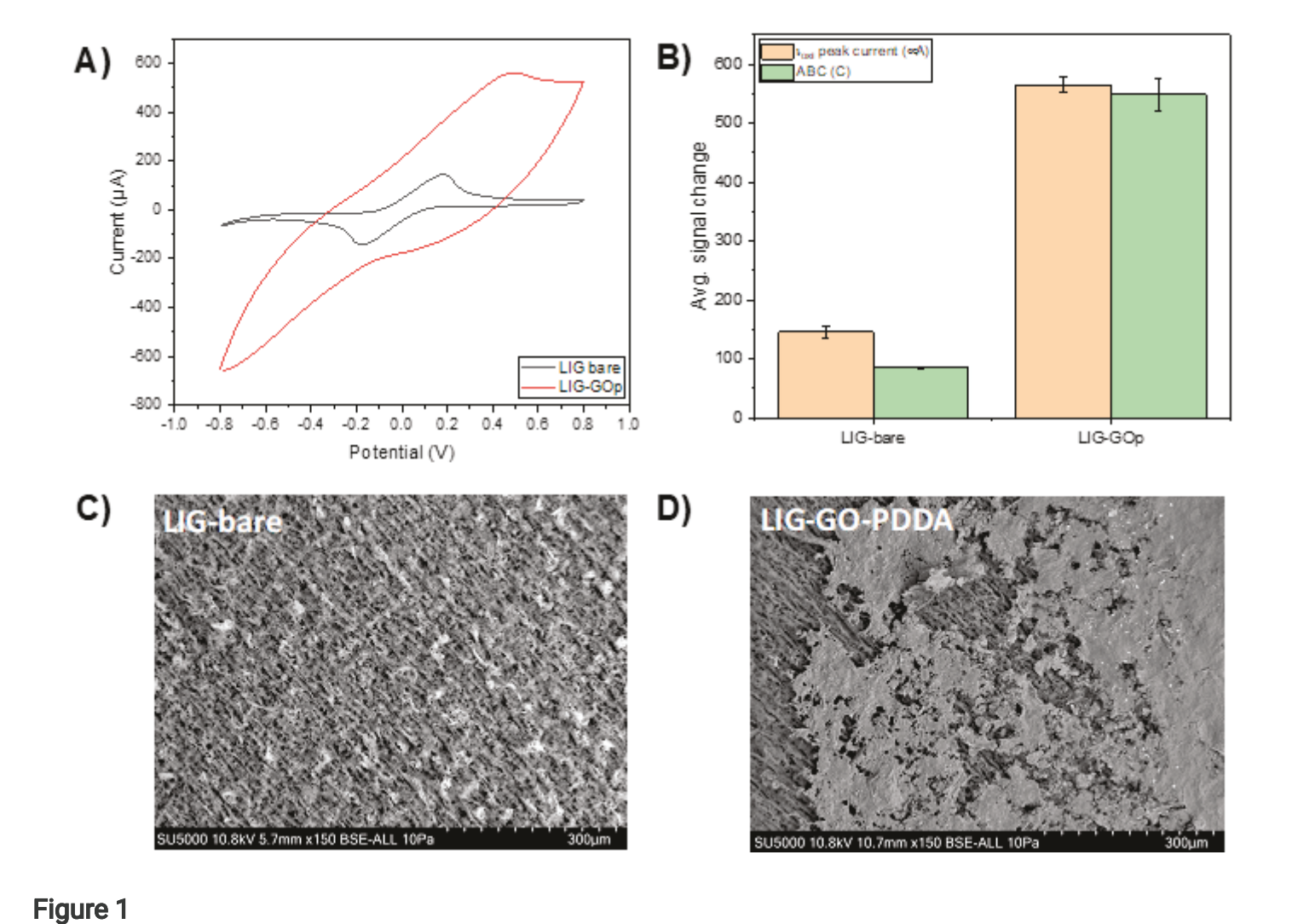
- 1. Brooks BW, Lazorchak JM, Howard MDA et al (2016) Are harmful algal blooms becoming the greatest inland water quality threat to public health and aquatic ecosystems? Environ Toxicol Chem 35:6–13. https://doi.org/10.1002/etc.3220
- 2. Stapanian MA, Schumacher W, Gara B, Monteith SE (2016) Negative effects of excessive soil phosphorus on floristic quality in Ohio wetlands. Sci Total Environ 551–552:556–562. https://doi.org/10.1016/j.scitotenv.2016.02.041
- 3. Penn CJ, Camberato JJ, Wiethorn MA (2023) How Much Phosphorus Uptake Is Required for Achieving Maximum Maize Grain Yield? Part 2: Impact of Phosphorus Uptake on Grain Quality and Partitioning of Nutrients. Agronomy 13:258. https://doi.org/10.3390/agronomy13010258
- 4. Hu B, Chu C (2020) Nitrogen-phosphorus interplay: old story with molecular tale. New Phytol 225:1455-1460. https://doi.org/10.1111/nph.16102
- 5. Anlauf A (2023) An extractive bioeconomy? Phosphate mining, fertilizer commodity chains, and alternative technologies. Sustain Sci 18:633–644. https://doi.org/10.1007/s11625-022-01234-8
- Akinnawo SO (2023) Eutrophication: Causes, consequences, physical, chemical and biological techniques for mitigation strategies. Environ Challenges 12:100733. https://doi.org/10.1016/j.envc.2023.100733
- 7. Shepherd JG, Kleemann R, Bahri-Esfahani J et al (2016) The future of phosphorus in our hands. Nutr Cycl Agroecosyst 104:281–287. https://doi.org/10.1007/s10705-015-9742-1
- 8. Cordell D, White S (2014) Life's Bottleneck: Sustaining the World's Phosphorus for a Food Secure Future. Annu Rev Environ Resour 39:161–188. https://doi.org/10.1146/annurev-environ-010213-113300

- 9. Alam MM, Srinivasan V, Mueller AV, Gu AZ (2021) Status and advances in technologies for phosphorus species detection and characterization in natural environment- A comprehensive review. Talanta 233:122458. https://doi.org/10.1016/j.talanta.2021.122458
- 10. Spangler C, Schaeferling M, Wolfbeis OS (2008) Fluorescent probes for microdetermination of inorganic phosphates and biophosphates. Microchim Acta 161:1–39. https://doi.org/10.1007/s00604-007-0897-6
- 11. McLamore E, Duckworth O, Boyer TH et al (2023) Perspective: Phosphorus monitoring must be rooted in sustainability frameworks spanning material scale to human scale. Water Res X 19:100168. https://doi.org/10.1016/j.wroa.2023.100168
- 12. Spivakov BY, Maryutina TA, Muntau H (1999) Phosphorus Speciation in Water and Sediments. Pure Appl Chem 71:2161–2176. https://doi.org/10.1351/pac199971112161
- 13. Bagyaraj DJ, Sharma MP, Maiti D (2015) Phosphorus nutrition of crops through arbuscular mycorrhizal fungi. Curr Sci 108:1288–1293. http://www.jstor.org/stable/24905490
- 14. U.S. Environmental Protection Agency (1986) United States Environmental Protection Agency. Quality criteria for water. https://nepis.epa.gov/Exe/ZyPDF.cgi/00001MGA.PDF?

 Dockey=00001MGA.PDF. Accessed 27 May 2024
- 15. Zimmerman Z, Keefe C (1997) Method 365.5 Determination of Orthophosphate in Estuarine and Coastal Waters by Automated Colorimetric Analysis. U.S. Environmental Protection Agency, Washington, DC
- 16. Nagul EA, McKelvie ID, Worsfold P, Kolev SD (2015) The molybdenum blue reaction for the determination of orthophosphate revisited: Opening the black box. Anal Chim Acta 890:60–82. https://doi.org/10.1016/j.aca.2015.07.030
- 17. Sivasankaran U, Reinke L, Anand SK et al (2020) Ultrasensitive electrochemical sensing of phosphate in water mediated by a dipicolylamine-zinc(II) complex. Sens Actuators B 321:128474. https://doi.org/10.1016/j.snb.2020.128474
- 18. Lu Y, Li X, Li D, Compton RG (2021) Amperometric Environmental Phosphate Sensors. ACS Sens 6:3284–3294. https://doi.org/10.1021/acssensors.1c01035
- 19. Prasad A, Sahu SP, Figueiredo Stofela SK et al (2021) Printed Electrode for Measuring Phosphate in Environmental Water. ACS Omega 6:11297–11306. https://doi.org/10.1021/acsomega.1c00132
- 20. Patel V, Selvaganapathy PR (2021) Enhancing the sensitivity of cobalt based solid-state phosphate sensor using electrical pretreatment. Sens Actuators B 349:130789. https://doi.org/10.1016/j.snb.2021.130789
- 21. Ye R, James DK, Tour JM (2018) Laser-Induced Graphene. Acc Chem Res 51:1609–1620. https://doi.org/10.1021/acs.accounts.8b00084
- 22. Soares RRA, Hjort RG, Pola CC et al (2020) Laser-Induced Graphene Electrochemical Immunosensors for Rapid and Label-Free Monitoring of Salmonella enterica in Chicken Broth. ACS Sens 5:1900–1911. https://doi.org/10.1021/acssensors.9b02345

- 23. Moreira G, Qian H, Datta SPA et al (2023) A capacitive laser-induced graphene based aptasensor for SARS-CoV-2 detection in human saliva. PLoS ONE 18:e0290256. https://doi.org/10.1371/journal.pone.0290256
- 24. Garland NT, McLamore ES, Cavallaro ND et al (2018) Flexible Laser-Induced Graphene for Nitrogen Sensing in Soil. ACS Appl Mater Interfaces 10:39124–39133. https://doi.org/10.1021/acsami.8b10991
- 25. Bahamon-Pinzon D, Moreira G, Obare S, Vanegas D (2022) Development of a nanocopper-decorated laser-scribed sensor for organophosphorus pesticide monitoring in aqueous samples. Microchim Acta 189:254. https://doi.org/10.1007/s00604-022-05355-w
- 26. Fu L, Lai G, Yu A (2015) Preparation of β-cyclodextrin functionalized reduced graphene oxide: application for electrochemical determination of paracetamol. RSC Adv 5:76973–76978. https://doi.org/10.1039/C5RA12520K
- 27. Casso-Hartmann L, Moreira GA, Tang Y et al (2024) Fabrication of laser inscribed graphene (LIG) 3-. https://doi.org/dx.doi.org/10.17504/protocols.io.dm6gpze1dlzp/v1. electrode plug-and-play chip
- 28. Brunetti BDE (2015) About Estimating the Limit of Detection by the Signal to Noise Approach. Pharm Anal Acta 06. https://doi.org/10.4172/2153-2435.1000355
- 29. Clogston JD, Patri AK (2011) Zeta Potential Measurement. In: McNeil SE (ed) Characterization of Nanoparticles Intended for Drug Delivery. Humana, Totowa, NJ, pp 63–70. https://doi.org/10.1007/978-1-60327-198–1_6
- 30. Qian H, Moreira G, Vanegas D et al (2024) Improving high throughput manufacture of laser-inscribed graphene electrodes via hierarchical clustering. Sci Rep 14:7980. https://doi.org/10.1038/s41598-024-57932-z
- 31. Vanegas DC, Patiño L, Mendez C et al (2018) Laser Scribed Graphene Biosensor for Detection of Biogenic Amines in Food Samples Using Locally Sourced Materials. Biosensors 8:42. https://doi.org/10.3390/bios8020042
- 32. Bakker E (1996) Determination of Improved Selectivity Coefficients of Polymer Membrane Ion-Selective Electrodes by Conditioning with a Discriminated Ion. J Electrochem Soc 143:L83. https://doi.org/10.1149/1.1836608
- 33. He Y, Han C, Du H et al (2024) Potentiometric Phosphate Ion Sensor Based on Electrochemically Modified All-Solid-State Copper Electrode for Phosphate Ions' Detection in Real Water. Chemosensors 12:53. https://doi.org/10.3390/chemosensors12040053
- 34. Ewaid SH, Abed SA (2017) Water quality index for Al-Gharraf River, southern Iraq. Egypt J Aquat Res 43:117–122. https://doi.org/10.1016/j.ejar.2017.03.001
- 35. Litke D (1999) Review of Phosphorus Control Measures in the United States and Their Effects on Water Quality. Geological Survey (U.S.)

Figures



Electrochemical and microscopic characterization of LIG before (LIG-bare) and after GO-PDDA (LIG-GO-PDDA) integration.

A) Representative voltammogram comparing LIG-bare and LIG-GO-PDDA in a solution of 100 mM KCl, 2.5 mM $K_3[Fe(CN)_6]/K_4[Fe(CN)_6]$ with a potential range from -0.8 to 0.8 V at 200 mV/s. **B)** Oxidation peak current (μ A) and Area Between Curve (C) before and after LIG functionalization with GOp. **C)** and **D)** Scanning Electron Microscopy (SEM) images of LIG-bare and LIG-GO-PDDA.

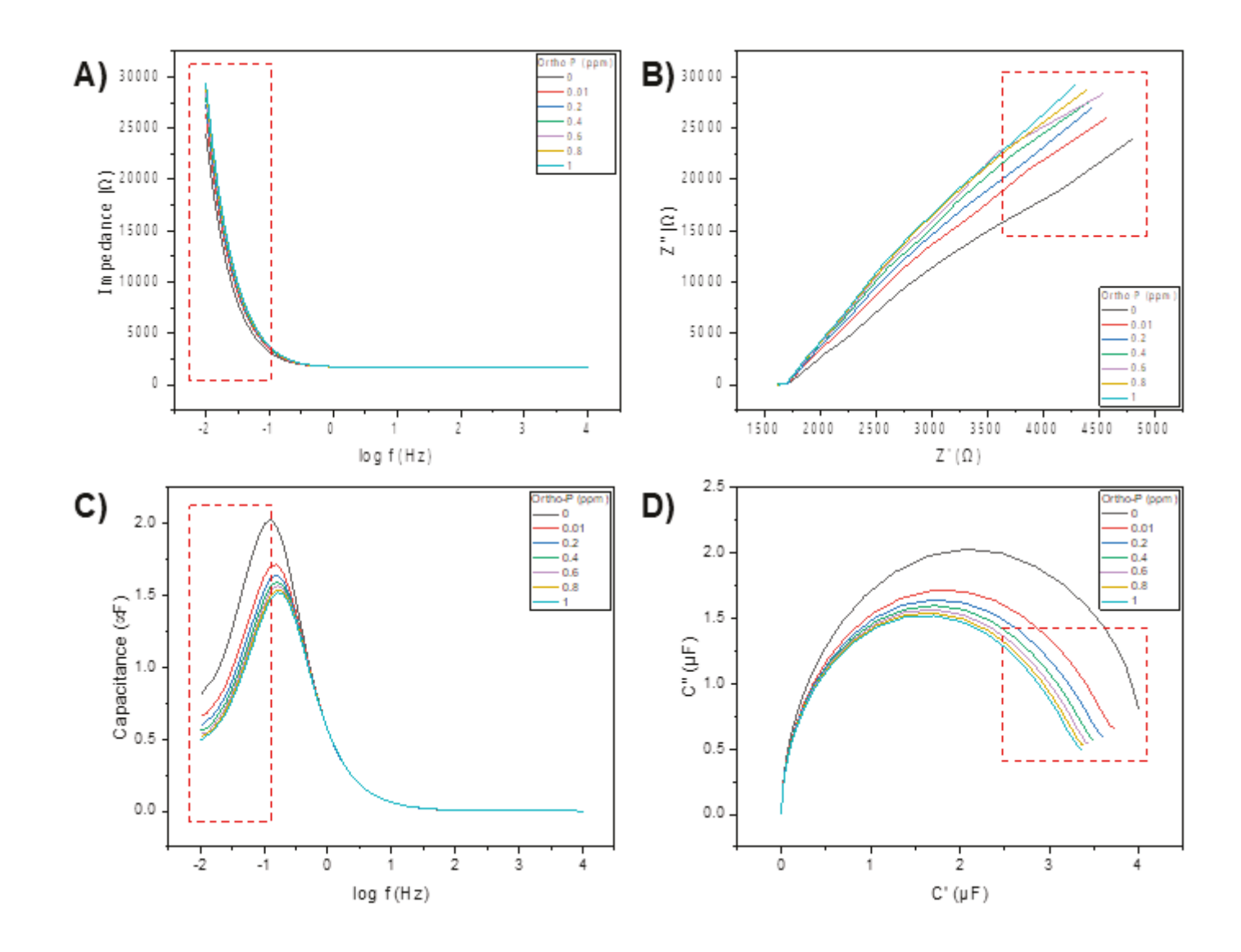


Figure 2 $Impedimetric \ and \ capacitive \ response \ for \ LIG-GO-PDDA \ in \ the \ presence \ of \ ortho-P \ (HPO_4^{2-}) \ in \ a \ sodium \ chloride/sodium \ bicarbonate \ solution \ (pH 8).$

A) Representative bode impedance plot (log f vs. Z). **B)** Representative Nyquist impedance plot (Z' vs. Z"). **C)** Representative bode capacitance plot (log f vs. C). **D)** Representative Nyquist capacitance plot (C' vs. C"). All the graphs show LIG-GO-PDDA response for increasing phosphate concentration from 0 to 1 ppm. The red square indicates a region of interest in each plot (approximately 0.01 to 1 Hz).

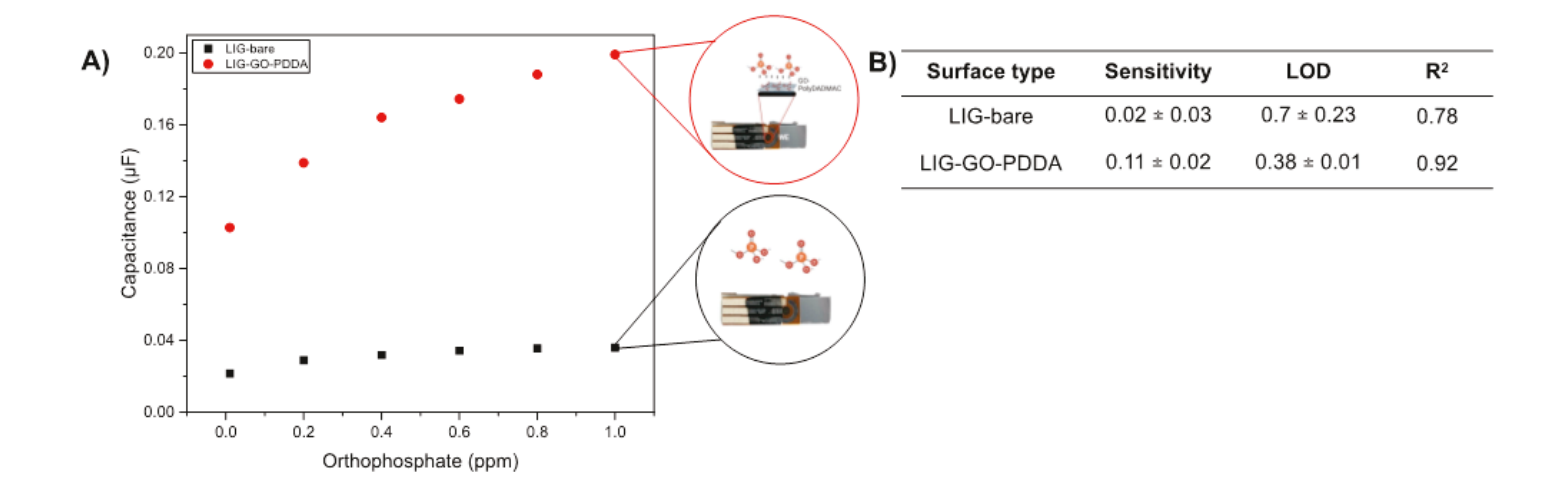
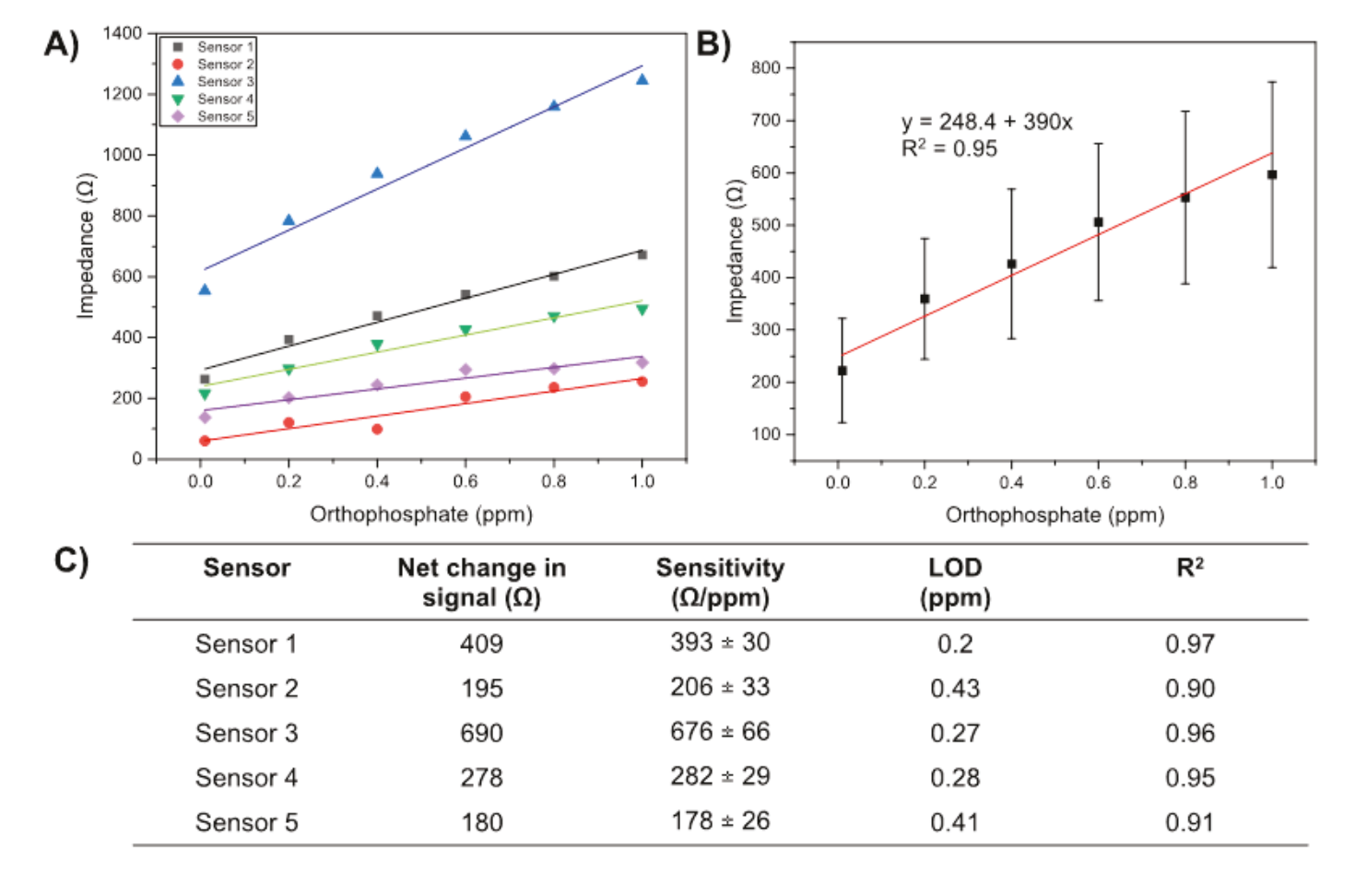


Figure 3

LIG surface comparison in response to ortho-P in a buffer.

A) Representative capacitive response of LIG-bare (black) and LIG-GO-PDDA (red) for increasing concentrations of ortho-P in buffer (pH 8). **B)** Performance metrics of LIG-bare and LIG-GO-PDDA in the presence of ortho-P (n=3). Capacitance was analyzed as a response variable at a frequency range from 0.01 to 1 Hz.



LIG-GO-PDDA sensor response for ortho-P in a buffer.

Figure 4

A) Representative impedimetric response of each LIG-GO-PDDA sensor for increasing ortho-P concentrations in buffer (pH 8). **B)** Calibration curve of LIG-GO-PDDA in the presence of ortho-P from mean measurements (n=5). **C)** Sensor performance metrics. Total impedance was analyzed as a response variable at a frequency range from 0.01 to 1 Hz.

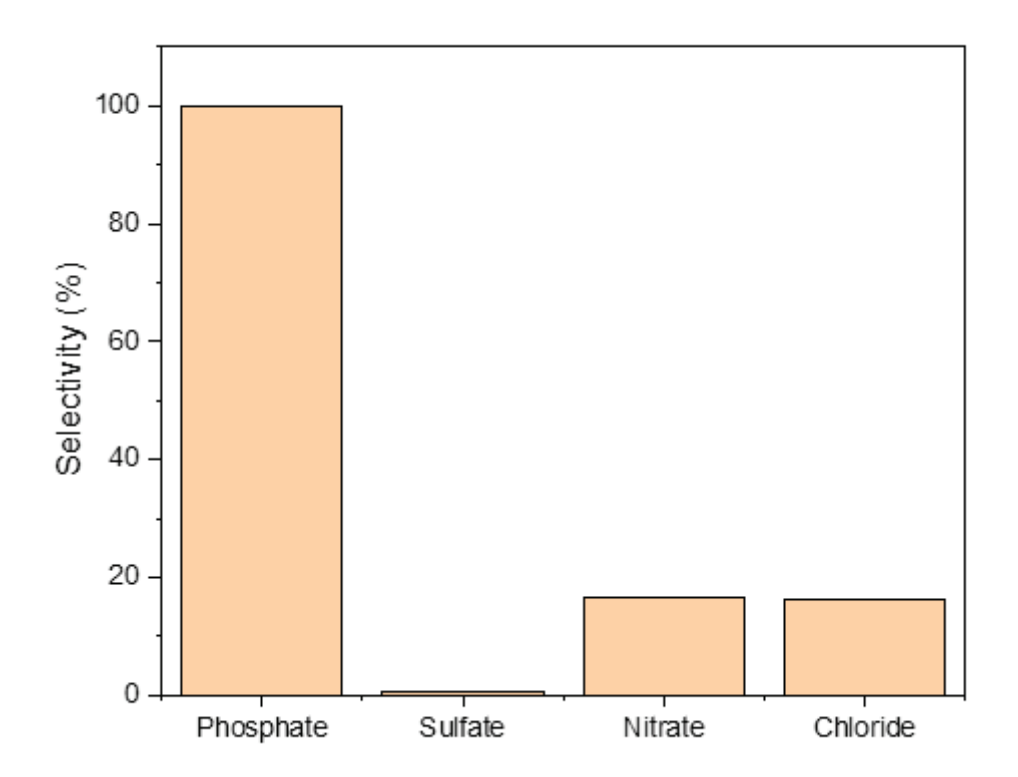
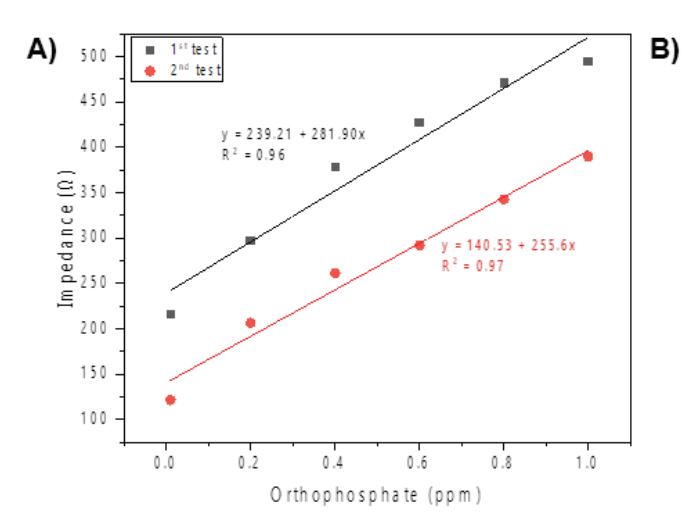


Figure 5

Selectivity performance (%) of LIG-GO-PDDA sensor towards phosphate, sulfate, nitrate and chloride.

Total impedance was analyzed by a ratiometric approach using frequencies 0.8 and 1.0 Hz.



Ortho-P	Sensor performance metrics (n=5)			
s ensing	S ens itivity (Ω/ppm)	Limit of detection (ppm)	R²	
1st test	389 ± 33	0.35 ± 0.06	0.95	
2 nd test	280 ± 16	0.6 ± 0.34	0.98	

Figure 6

Sensor performance before and after regeneration with an acidic buffer (pH 5).

A) Representative calibration curve of LIG-GO-PDDA sensor for increasing ortho-P concentration (0 to 1 ppm) before (1st test, black) and after (2nd test, red) sensor regeneration with an acidic buffer (pH 5). **B)** Performance metrics of the sensor before and after regeneration (n=5).

Supplementary Files

This is a list of supplementary files associated with this preprint. Click to download.

• MoreiraetalMicrochimicaActa063024supplemental.docx